

Computing Electromagnetic Fields in Inhomogeneous Media Using Lattice Gas Automata

M.Zhang, D. Cule[△], L. Shafai, G. Bridges and N.Simons[†]

Department of Electrical and Computer Engineering
University of Manitoba
Winnipeg, Canada R3T 5V6

[△]VPRS, [†] Directorate of Antennas and Integrated Electronics
Communications Research Centre
Ottawa, Canada K2H 8S2

I. Introduction

Lattice Gas Automata (*LGA*) can be considered as an alternative to the conventional differential equation description of problems in electromagnetics. *LGA*s are discrete dynamical systems that are based on a microscopic model of the physics being simulated. The basic constituents of an *LGA* are discrete cells. These cells are interconnected according to certain symmetric requirements to form an extremely large regular lattice. The cells of an *LGA* are extremely simple, requiring only a few bits to completely describe their states. Even though they are simple however, the collective behaviour of *LGA* microscopic systems are capable of exhibiting those behaviours described by partial differential equations for real physical systems. One type of simple *LGA*, the *HPP LGA*, is constructed with only a few bits per cell and operated on a rectangular lattice. We have demonstrated [1] that it is capable of simulating two dimensional electromagnetic fields. Furthermore, the inherent parallelism and simplicity of *LGA* algorithms make them ideally suited to implementation in a parallel processing architecture.

In this paper we present new *HPP*-type mixture *LGA* algorithms for modelling wave propagation in inhomogeneous dense media. Change in sound speed of an *LGA* can be achieved by incorporating rest bits at a lattice site as well as moving or interaction bits. We analytically show how this model can be applied to the simulation of electromagnetic fields in inhomogeneous media. In this paper our analysis is based on the more complex hexagonal lattice with results presented for a rectangular (*HPP*) lattice shown in Fig.1. With the small perturbation assumption, we develop and check the validity of a simple *HPP* model for simulating wave propagation. The ability to model media with different sound speeds is analogous to modelling different dielectric constants in inhomogeneous media of electromagnetics. We theoretically give a general formula for the sound speed which enables a wide range of dielectric constant to be modelled by specifying various interaction models in an *LGA*. A variety of applications of this model for problems of wave interaction with dielectric objects, from a simple heterogeneous dielectric cylinder to complex biological structures, are reported and compared with traditional numerical methods.

II. Lattice Gas Automata and Mixture Model

An *LGA* model without zero-velocity “rest particles” can only yield a uniform sound speed. To enable the *LGA* lattice to model media with different sound speeds (analogous to modelling different dielectric constants in electromagnetics), certain rest particles are incorporated within sites of the lattice. It will be seen in the analysis that there are only a few restrictions (conservations of mass and momentum, and semi-detail balance) imposed on constructing such mixture models, and thus there are many ways for them to be employed. One can also specify that certain regions of the lattice have different rest particle numbers and masses. The energy exchanges between moving and rest particles in the regions are thus different, and a lattice with inhomogeneous sound speeds can be realized.

Fig.2 shows two example cells of our mixture models, one for a rectangular (*HPP*) lattice and the other for a hexagonal (*FHP*) lattice [2]. Except for the moving particles (4 moving particles associating with a *HPP* cell, 6 moving particles with a *FHP* cell), there are up to b_r rest particles allowed at a lattice site. We denote these b_r rest particles to be m_1, m_2, \dots, m_{b_r} , respectively. To obtain a spatial distribution of sound speeds on the lattice, b_r is then defined to be a function of position. A completely arbitrary sound can then be specified by creating mixtures of cells with different rest particle numbers by using a weight parameter p_k^p ($k = 1, \dots, b_r$), where p_k^p is the creation or annihilation probability of rest particle m_k . In Fig.3, one of many rest particle models are shown, where a stack ($b_r = 3$) of particles of various masses ($m_1=4, m_2=8$ and $m_3=16$) can be created. Exchange of energy between moving and rest particles occurs when a rest particle of mass 4 is created when four unit mass moving particles collide and where there is initially no mass 4 rest particle. Alternatively, if a mass 4 rest particle already exists at a site, and there are no initial moving particles, four moving particles will be created after the collision phase, and the rest particle will be annihilated. Even more generally, we could incorporate stochastic rules which probabilistically allow rest particles to be created or annihilated

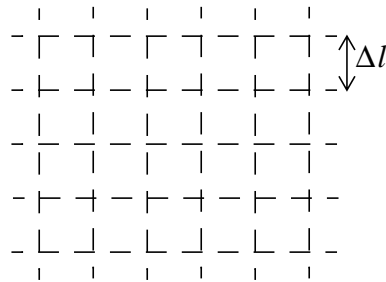


Fig.1: *HPP* lattice with rectangular cells.

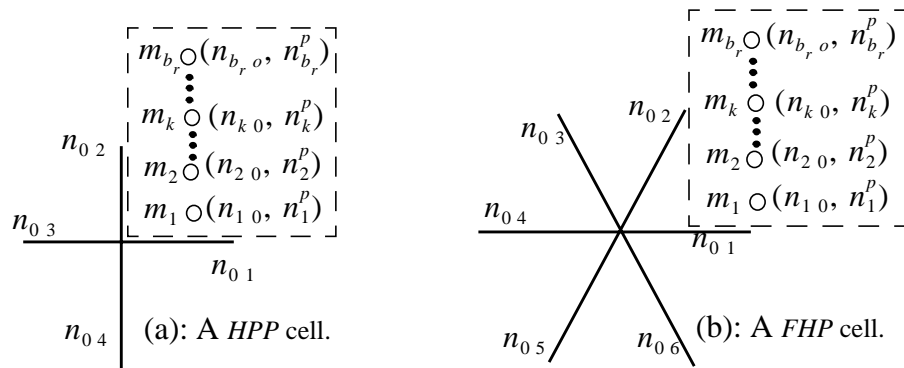


Fig.2: *LGA* rule with b_r probabilistically weighted rest particles: (a): *HPP* mixture model, (b): *FHP* mixture model.

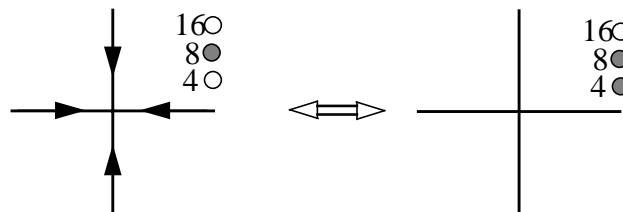


Fig.3: *LGA* rule with three weighted rest particles.

In the analysis of this model we will use two subscript binary variables $n_{i,k}(\mathbf{x}, t)$ to represent the particle states at a particular site \mathbf{x} and time step t in the mixture lattice. In this notation the first subscript i represents the velocity direction of particles. Thus, the moving particles in a particular cell can be denoted as $n_{i,0}(\mathbf{x}, t)$, where $i=1,2,3$ and 4 for the four moving particles of the *HPP* model, and $i=1,\dots,6$ for the six moving particles of the *FHP* model, and $i=0$ for rest particles. The second subscript k represents the mass index of the particles. For moving particles (unit mass) $k \equiv 0$. Following the notation, the bits $\{n_{o,k}, k = 1 \dots b_r\}$ represent the rest particles with mass m_k . The random bit variables $n_k^p (k = 1 \dots b_r)$ are introduced to stochastically describe the presence or absence of a rest particle- $s m_k (k = 1 \dots b_r)$ at a lattice site. These bits $n_k^p (k = 1 \dots b_r)$ are randomly sampled with the average values of $\langle n_k^p \rangle = p_k^p (k = 1 \dots b_r)$, and satisfying the limitations $p_{k+1}^p \leq p_k^p$ and $\sum_{k=1}^{b_r} p_k^p \leq 1$.

III.Theoretical Analysis

Considering the exclusion of viscosity in the final analysis, we begin with the more complex *FHP* lattice and then later limit it to the Euler equation derived from the lowest order of the Chapman-Enskog expansions[3]. The *FHP* lattice is used since it enables a more rigorous analysis. The microscopic dynamics can be expressed in terms of the bit variables for the moving particles as

$$n_{i,o}(\mathbf{x} + \mathbf{c}_i, t + \Delta t) = n_{i,o}(\mathbf{x}, t) + \omega_{i,o}[n^\dagger(\mathbf{x}, t)] \quad (i = 1, \dots, b_m), \quad (1)$$

and for the rest particles as

$$n_{o,k}(\mathbf{x}, t + \Delta t) = n_{o,k}(\mathbf{x}, t) + \omega_{o,k}[n^\dagger(\mathbf{x}, t)] \quad (k = 1, \dots, b_r), \quad (2)$$

where c_i represents the velocity states in which the moving particles at a site might exit, and where $b_m=6$ for the *FHP* and $b_m=4$ for *HPP* lattice. The collision operator $\omega_{i,k}(n^\dagger)$ describes the change in bits due to collisions. The symbol $\omega(n^\dagger(\mathbf{x}, t))$ indicates the dependency of the collision operator on all bit variables $n_{i,k}$ at site \mathbf{x} and timestep t . The macroscopic understanding of the lattice dynamic system can be obtained by performing an ensemble average by assuming Boltzmann molecular chaos assumption. The Boltzmann equations in terms of the mean population of particles $N_{i,k} = \langle n_{i,k} \rangle$ can then be obtained as

$$N_{i,o}(\mathbf{x} + \mathbf{c}_i, t + \Delta t) = N_{i,o}(\mathbf{x}, t) + \Omega_{i,o}[N^\dagger(\mathbf{x}, t)] \quad (i = 1, \dots, b_m), \quad (3)$$

$$N_{o,k}(\mathbf{x}, t + \Delta t) = N_{o,k}(\mathbf{x}, t) + \Omega_{o,k}[N^\dagger(\mathbf{x}, t)] \quad (k = 1, \dots, b_r), \quad (4)$$

where $\langle \omega(n^\dagger) \rangle \approx \Omega(\langle n^\dagger \rangle) \approx \Omega(N^\dagger)$, and N^\dagger indicates that the dependency of the collision operator $\Omega(N^\dagger)$ on all the mean population of particles $N_{i,k}$. To obtain a solutions for the above equation and understand the macroscopic behaviour, a Chapman-Enskog perturbation expansion and multi-scale technique [2] can be utilized. In order to this we first consider the solutions for equations (3) and (4) at local equilibria with density and momentum slowly changing in space and time. It can be proved [2,4] if the collisions verify the semi-detailed balance and conserve mass and momentum, the mean population of particle at equilibria $N_{i,k}^{eq}$ are described by the *Fermi-Dirac* distribution. By using the conservation of mass and the conservation of momentum,

$$\rho = \sum_{\substack{i=1 \\ (k=0)}}^{b_m} N_{i,o}^{eq} + \sum_{\substack{k=1 \\ (i=0)}}^{b_r} m_k N_{o,k}^{eq} p_k \quad (5)$$

$$\rho \mathbf{u} = \sum_{\substack{i=1 \\ (k=0)}}^{b_m} N_{i,o}^{eq} \mathbf{c}_i \quad (6)$$

where ρ and \mathbf{u} are the mass density and flow velocity per cell, respectively. The filling ratio p_k is related to the initial condition, representing that in this mixture model p_k sites on the lattice are initialized with rest particle of mass m_k . The random bit probability of p_k^r is related to the local collision rules. The equilibrium solution for moving and rest particles can be obtained as

$$N_{i,o}^{eq} = d \left\{ 1 + \frac{2\rho}{c^2 \rho_m} \mathbf{c}_i \cdot \mathbf{u} + \frac{2\rho^2 (1-2d)}{c^4 \rho_m^2 (1-d)} \left[c_{i\gamma} c_{i\delta} - \frac{c^2}{2} \delta_{\gamma\delta} + \left(\frac{c^2}{2} - c_s^2 \right) \delta_{\gamma\delta} \right] u_\gamma u_\delta \right\}, \quad (7)$$

$$N_{o,k}^{eq} = d_k \left[1 - \frac{2\rho^2 (1-2d)}{c^4 \rho_m^2 (1-d)} \frac{(1-d_k)}{(1-d)} u^2 m_k c_s^2 \right] \quad (8)$$

In the above expressions, Greek index represents the spatial components of velocity of the particles. At the equilibrium the average moving particle density d and the rest particle density d_k with mass m_k can be related by $d_k = d^{m_k} / \left(d^{m_k} + (1-d)^{m_k} \right)$. c_s is the sound speed of the lattice to be determined latter.

Now, to obtain the perturbation solution to the Boltzmann equations (3) and (4) near equilibria we expand $N_{i,k}$ around the equilibria as a series in powers of ϵ [2,4]

$$N_{i,k} = N_{i,k}^{(o)} + N_{i,k}^{(1)} + N_{i,k}^{(2)} + O(\epsilon^3), \quad (9)$$

where $N_{i,k}^{(o)} = N_{i,k}^{eq}$. Based on Chapman-Enskog expansion, a multi-scale technique is used by assuming that the gradients of the $N_{i,k}^{(n)}$ and the related time ∂t are very small, thus satisfying $\nabla \sim \partial t = O(\epsilon)$ for the first order derivative and $\nabla^{(n)} = O(\epsilon^n)$ for the n th order derivative.

Now we insert the expansion (7) in the Boltzmann equations (3) and (4) and use the above multi-scale technique. By identifying the terms at order $O(\epsilon)$, the following equations can be written for the first order solutions of $N_{i,o}^{(1)}$ and $N_{o,k}^{(1)}$, respectively,

$$\partial_t N_{i,o}^{(o)} + c_{i\beta} \partial_\beta N_{i,o}^{(o)} = \sum_{j=1}^{b_m} \Lambda_{ij}^m N_{j,o}^{(1)} + \sum_{k=1}^{b_r} \Lambda_{i,k}^m N_{o,k}^{(1)}, \quad (10)$$

$$\partial_t N_{o,k}^{(o)} = \sum_{l=1}^{b_r} \Lambda_{k,l}^r N_{o,l}^{(1)} + \sum_{j=1}^{b_m} \Lambda_{k,j}^r N_{j,o}^{(1)}, \quad (11)$$

$$\Lambda_{i,j}^m = \left(\frac{\partial \Omega_{i,o}}{N_{j,o}} \right) \Big|_{N^\dagger = N^{\dagger eq}}, \quad \Lambda_{i,k}^m = \left(\frac{\partial \Omega_{i,o}}{N_{o,k}} \right) \Big|_{N^\dagger = N^{\dagger eq}}, \quad \Lambda_{k,l}^r = \left(\frac{\partial \Omega_{o,k}}{N_{o,l}} \right) \Big|_{N^\dagger = N^{\dagger eq}}, \quad \Lambda_{k,j}^r = \left(\frac{\partial \Omega_{o,k}}{N_{j,o}} \right) \Big|_{N^\dagger = N^{\dagger eq}}.$$

It can be shown that by using the conservations of mass and momentum (5) and (6), the macroscopic equations for mass and momentum can be written as

$$\partial_t \rho + \nabla \cdot (\rho \mathbf{u}) = 0 \quad (12)$$

$$\partial_t (\rho \mathbf{u}) + \nabla \cdot (\rho g(\rho) \mathbf{u} \mathbf{u}) = -\nabla P(\rho, u^2) \quad (13)$$

$$(\rho, u^2) = \frac{\rho_m c^2}{2} - \rho \frac{1}{2} \frac{\rho}{\rho_m} \frac{1-2d}{1-d} \frac{c_s^2}{c^2} \left(2 - \frac{1}{2} \frac{c^2}{c_s^2} \left(1 + \frac{1}{2} \right) \right) \quad (14)$$

$$\rho_m = b_m d \quad , \quad \rho_r = \sum_{k=1}^{b_r} m_k p_k d_k \quad (15)$$

Equations (12)-(15) show that the first order perturbation on the lattice obey the Euler equation. To determine the linear wave behaviour of the lattice and associated sound speed c_s , we consider a case in which a small perturbation (ρ', \mathbf{u}') is superposed onto an equilibrium state with density ρ_o and zero flow $\mathbf{u}_o = \mathbf{0}$. We can write $\rho \approx \rho_o + \rho'$ and $\mathbf{u} \approx \mathbf{u}'$, where ρ_o is the uniform background density, ρ' and \mathbf{u}' are, respectively, weak density and flow perturbation with the order of $O(\epsilon)$. For this situation, the conservation of mass and mass at order $O(\epsilon)$ can be expressed as

$$\partial_t \rho' + \rho_o \nabla \cdot \mathbf{u}' = 0, \quad (16)$$

$$\partial_t \mathbf{u}' + c_s^2 / \rho_o \nabla \rho' = 0, \quad (17)$$

where the parameter, the sound speed c_s , is calculated from (17) as

$$c_s^2 = \left(\frac{\partial P}{\partial \rho} \right) \Big|_{u=0} = \frac{c^2}{2} \left(\frac{\partial \rho_m}{\partial \rho} \right) \Big|_{u=0} = c^2 b_m d (1-d) / \left(2 \left[b_m d (1-d) + \sum_{k=1}^{b_r} m_k^2 p_k d_k (1-d_k) \right] \right) \quad (18)$$

Equations (16) and (17) can be combined to eliminate \mathbf{u}' and lead to the linear wave equation in terms of ρ' as

$$\partial_t^2 \rho' - c_s^2 \nabla^2 \rho' = 0 \quad (19)$$

Here we can note that the regime of undamped sound wave involves only the lower symmetric requirements [2,4], and thus the simple rectangular lattice of *HPP* is valid for modelling linear wave propagation.

An analogy now can be made between the above two-dimensional wave equation (19) and two-dimensional *TM* or *TE* electromagnetic fields. For the *TM_z* case, the macroscopic perturbative density, can be equated to the electric field E_z , and the x- and y- components of the perturbative flow velocity, $\mathbf{u}' = (u'_x, u'_y)$, ρ' can be equated to magnetic field components, H_y and H_x , respectively. Similarly, for the case of *TE_z*, ρ' can be equated to the magnetic field H_z , and $\mathbf{u}' = (u'_x, u'_y)$ can then be equated to electric field components E_y and E_x respectively. In addition to this analogy, the mixture *HPP* enables us to control the sound speed (dielectric constant) in a very flexible way.

IV. Numerical Results

Several results are then presented as examples of the mixture *HPP LGA* for modelling inhomogeneous dielectric media in two-dimensional electromagnetic problems. Fig.4 shows the time-domain scattering intensity inside a dielectric cylindrical shell with $\epsilon_r = 5$ and of inner radius $a=80 \Delta l$ and outer radius $b=100 \Delta l$. The shell was created using a single rest particle $m_1 = 4$. Fig.5 demonstrates a gaussian plane propagating through a dielectric cylindrical shell with $\epsilon_r = 85$. To obtain a relative dielectric constant

$\epsilon_r = 85$, a mixture model with up to three rest particles with masses $m_1 = 4$, $m_2 = 8$, and $m_3 = 16$ was constructed. As an example of wave interaction with a complex biological structure, the scattering field from a human body cross-section model (dielectric values only) was simulated and shown in Fig.6. In this body cross-section model more than eight tissues with different dielectric constants ranging from 4 to 85 were modelled.

V. Conclusion

We have presented and analysed a new LGA mixture model for inhomogeneous media. As indicated by the sound speed formula (18), only with a few restrictions on such things as the conservation laws and the semi-detailed balance condition, there are a great number of the collision rules which are qualified to specify the lattice to enable a wide range of dielectric constant to be modelled. This has been confirmed by a variety of simulation experiments[5].

VI. References

- [1] N.R.Simons, G. Bridges, B.Podaima and A.Sebak, "Cellular Automata as Environment for Simulating Electromagnetic Phenomena", *IEEE Microwave and Guided Wave letters*, vol.4, pp.247-249,1994.
- [2] U.Frisch, D.d'Humieres, B.Hasslacher, P.Lallemand, Y.Pomeau and J.P.Rivert, "Lattice Hydrodynamics in two and three dimensions", *Complex Syst.* vol.1, pp. 649-707, 1987.
- [3] S.Chapman and T. Cowling, "The Mathematical Theory of Non-Uniform Gases", 3rd.ed., Cambridge University, Cambridge, England,1970.
- [4] D.Rothman and S.Zaleski, "Lattice-Gas models for Phase Separation: Interface, Phase Transitions and Multiphase Flow", *Rev. of Modern Phys.*, vol.66, No.4, pp. 1417-1479,1994.
- [5] G. Bridges, N.R.Simons, D.Cule, M. Zhang and M.Cuhaci, "Application of the Lattice Gas Automata Technique to modelling Wave Interaction with Biological Media", *Proceedings of the IEE10th International Conference Antennas and Propagation*, vol.2, pp.2.286-2.289, April, 1997.
- [6] P.B. Johns, "A Symmetric Condensed Node for the TLM Method," *IEEE Trans. Microwave Theory and Techniques*, vol.35, No.4, pp. 370-377, April 1987.

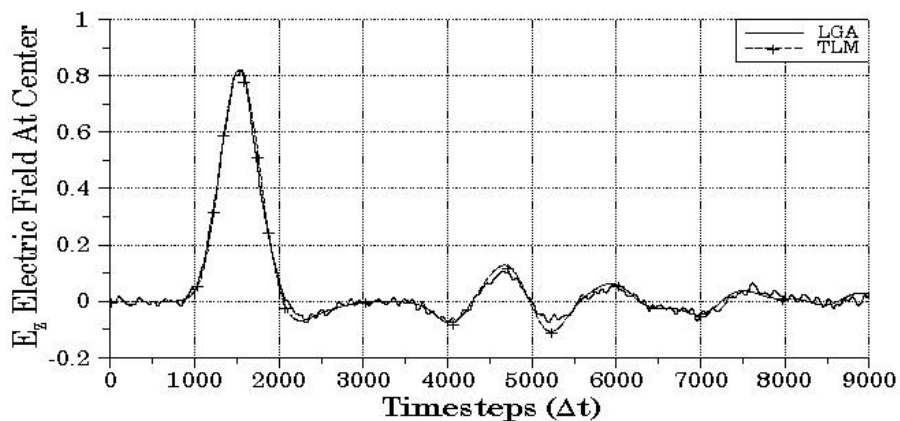


Fig.4: Time-domain field intensities for the electric field intensity inside a dielectric cylindrical shell with $\epsilon_r = 5$. Comparison is made to the results obtained using the TLM method[6].

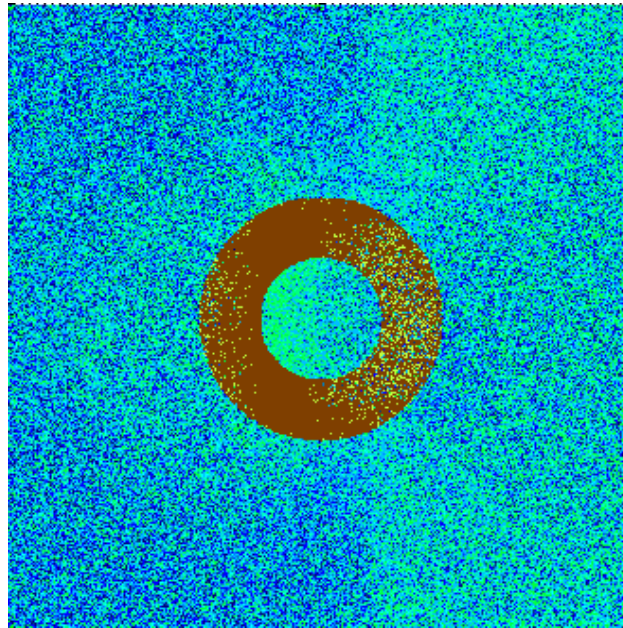


Fig.5: Snapshot of the microscopic field intensity for a gaussian plane wave propagating through a dielectric cylindrical shell with $\epsilon_r = 85$.

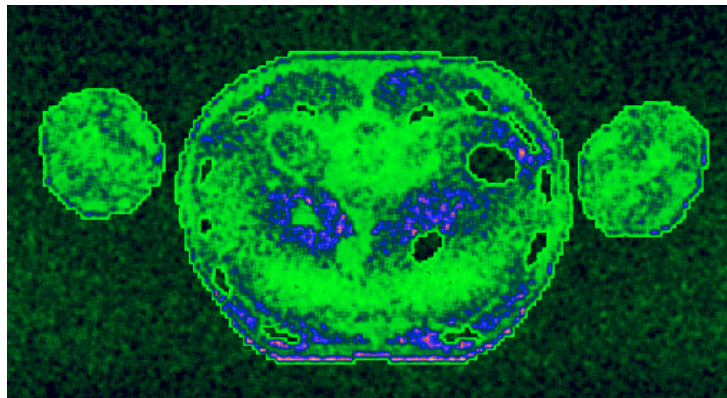


Fig.6: Image of the instantaneous field intensity for harmonic plane wave incidence on the the cross section of human torso at 975 MHz .